Journal of New Materials for Electrochemical Systems 15, 301-306 (2012)

Electrochemical Behavior of (Zn, Mn)-Al Nitrated Hydrotalcites

Alvaro Sampieri[1,*], Jorge Vázquez-Arenas[2], Ignacio González[3], Geolar Fetter[4], Heriberto Pfeiffer[5], María-Elena Villafuerte[5] and Pedro Bosch[5]

[1]Benemérita Universidad Autónoma de Puebla, Facultad de Ingeniería Química, Ciudad Universitaria, 72570, Puebla, PUE, Mexico.
[2]Chemical Engineering Department, University of Waterloo, 200 University Avenue West, Waterloo, Ontario, Canada N2L 3G1.
[3]Universidad Autónoma Metropolitana-Iztapalapa, Departamento de Química, A. P. 55-534, 09340 Mexico D.F., Mexico.
[4]Benemérita Universidad Autónoma de Puebla, Facultad de Ciencias Químicas, Ciudad Universitaria, 72570, Puebla, PUE, Mexico.
[5]Instituto de Investigaciones en Materiales, Universidad Nacional Autónoma de México, A.P. 70360, Ciudad Universitaria, 04510 Mexico, D.F., Mexico

Received: March 14, 2012, Accepted: April 17, 2012, Available online: May 22, 2012

Abstract: *The electrochemical behavior of synthetic binary, Zn-Al and Mn-Al, and ternary (Zn-Mn)-Al hydrotalcites (HT) was studied by cyclic voltammetry in alkaline conditions (pH≡12). The Zn-Al HT characterization revealed two irreversible and continuous oxidation processes: i) $Zn^0|Zn^{2+}$ and ii) $Zn^0|ZnO$. On the other hand, the binary HT containing Mn presented a reversible behavior for the oxidation-reduction process $Mn^{4+}|Mn^{3+}$. The same oxidation-reduction processes were observed in the ternary HT. However, variations in the reduction-oxidation process were detected by XRD for the ternary HT as a result of spinel formation. These results could also be influenced due to a higher accessibility of manganese in HT since the morphology of hydrotalcite (lamellar structure) provides a regular distribution of Mn atoms interacting with Zn atoms through hydroxyl bridges.*

Keywords: Electroactive hydrotalcites, Cyclic voltammetry, morphology

1. INTRODUCTION

Electron transfer in hydrotalcites (HT) relies upon the chemical properties of their surface. Novel applications in electrocatalysis and electroanalysis demand improving their electron transfer by attaching electroactive species to these surfaces. Accordingly, their performance is paramount for the efficiencies obtained for electrochemical applications (1). To this concern, the modification of these interfaces can be performed through a variety of methods: adsorption, covalent bonding, polymer wilt-film coverage, coverage with particles of nonconducting solids, etc. Considerable work has been reported on electrode modification with non-conductive materials, such as zeolites (2), hydrotalcites and cationic clays (3) since they have the ability to incorporate ions by exchange processes.

Hydrotalcites (HT) are layered double hydroxide minerals. They can be natural or synthetic anionic clays with positively charged layers balanced by hydrated anions(1) In general, HT composition is defined by the formula $[M^{2+}_{1-x}M^{3+}_x(OH)_2][A_n^{-x/n}\cdot mH_2O]$, with x = molar ratio $M^{3+}/(M^{2+}+M^{3+})$ and $0.2 < x < 0.33$. The layered structure is usually constituted by octahedrally coordinated divalent (Mg^{2+}, Ni^{2+}, Zn^{2+} …) and trivalent (Al^{3+},Fe^{3+} …) cations, sharing edges to form infinite brucite-like sheets, $Mg(OH)_2$. The interlayer space may be occupied by CO_3^{2-}, NO_3^-, Cl^-, etc. (4, 5) or more complex anions (4) as $Fe(CN)_6^{3,4-}$, $V_2O_7^{6-}$, $Mo_7O_{24}^{6-}$. Hydrotalcites are versatile materials since their properties can be modulated by changing the nature of the M^{2+} and M^{3+} cations, *i.e.* altering the brucite like layer charge.

The most common hydrotalcite is constituted by magnesium and aluminum, whereby it is not electronically conductive. Modifications in their structure with bivalent transition metals have been proposed (2) to improve the electrochemical accessibility of species adsorbed on HT-modified electrodes and alleviate this problem. Table 1 summarizes some HT compounds formerly used for electrodes, sensors or biosensors, and electrocatalysts. Roto *et al*. (6-8) have shown that electrodes modified with Ni/Al, Co/Al or

*To whom correspondence should be addressed: Email: asamcr@yahoo.com

Mg/Mn HTs are electroactives. Likewise, Oliver-Tolentino *et al*., (9) have recently prepared Mg/Al and Mg/Ca/Al hydrotalcites immersed in a carbon paste electrode matrix to obtain the so-called modified carbon paste electrode (CPE), and thus, improving the electrochemical oxidation of blue 69 dye. Indeed, CPE is a practical alternative to characterize the activity of the electrode by means of voltammetry (10,11). CPE is made up of graphite powder and a nonconducting liquid binder. The main advantage of these electrodes is the possibility to renew the active surface after each experiment (e.g. only removing the portion of used material). Moreover, CPEs have a high capacity for specific accumulation of electroactive compounds and provide a homogeneous material dispersion.

Thus, the aim of this work is to analyze the reaction mechanism of electrodes modified with (Zn or/and Mn)-Al hydrotalcites enclosing binary and ternary cations in the HTs. Modified CPEs were prepared containing these HTs to characterize their electrochemical behavior. Cyclic voltammetry was used to characterize the ionic and electronic response of the (Zn or/and Mn)-Al hydrotalcite-like compounds under alkaline conditions (pH ≡12), and the effects arising from the M^{2+} metal interactions.

2. EXPERIMENTAL

Hydrotalcite preparation. Binary hydrotalcites composed by Zn^{2+}-Al and Mn^{2+}-Al were synthesized by coprecipitation (12) with a M^{2+}/Al^{3+} molar ratio of 2/1. Two aqueous solutions, one containing hydrated salts of $Mn(NO_3)_2$ from Aldrich, 98% (or $Zn(NO_3)_2$) and $Al(NO_3)_3$ from Aldrich, 99%, and the other NaOH (1.85 M) from Baker, 98%, were added dropwise into a flask at room temperature. In order to avoid the ZnO formation in the Zn-Al HT, the pH was maintained between 7.5 and 8.5 (13, 14). After precipitation, samples were irradiated in a microwave oven (MIC-I, Sistemas y Equipos de Vidrio, S. A. de C. V.) operating at 200 W for 10 min to accelerate condensation and crystallization steps (15). The maximal temperature reached into the reactor was 353 K. The mixture final volume was about 400 ml to obtain *ca*. 20 g of dried product. Prior to drying at 343 K for 24 h, the precipitates were washed with deionized water. The same procedure was used to prepare a ternary HT containing (Zn-Mn),-Al keeping the $[Zn^{2+}$-$Mn^{2+}]/Al^{3+}$ nominal ratio equal to 2.

HTs characterization. X-ray diffraction (XRD) patterns were recorded with a Bruker axs D8 advance diffractometer coupled to a copper anode X-ray tube. To calculate *a* and *c* cell HT parameters, NaCl was used as internal reference. X-ray energy dispersive analyses (EDX) were performed in a Cambridge Leica Stereoscan 440 microscope. Samples were previously coated with gold to avoid the lack of conductivity.

2.1. Reagents for electrode preparation

Graphite powder, 2–5 μm particle size, was purchased from Alfa AESAR™ (99.9995% purity). It was used as supplied with no further purification. Liquid binders of high purity were used: silicone oil was purchased from Sigma, with 0.963 g/mL density, 400 cp viscosity, (refraction index) nD= 1.4058.

2.2. Preparation of carbon paste electrode (CPE)

0.2 g of HT was mixed with 0.3 g of graphite and 0.25 mL of silicon-oil. These compounds were mixed for 30 min in an agate

Table 1. Some studies reporting the use of hydrotalcites as electroactive materials.

M^{2+}_{1-x}–M^{3+}_{x}	$A^{n-}_{x/n}$	Study	Year	Author
Co-Al Ni-Al	Cl^-, CO_3^{2-}, SO_4^{2-}	Pt modify electrodes	2006/2005	Scavetta *et al.* (21, 22) Ballarin *et al.*(23)
Ni-Al	$[Fe(CN)_6]^{4-}$	A^{n-} adsorption	2004	Carpani et al.(24)
Zn–Cr	Azinobisethyl-benzothiazoline	Biosensors	2004	Shan *et al*. (25)
Zn-Cr	Cl^-, CO_3^{2-}	Electrokinetics	2004	Rojas Delgado *et al.* (26)
Ni-Al	Cl^-	Sensors	2001	Scavetta *et al.* (27)
Mg–Al	Cl^-, NO_3^-	Potentiometry	2000	Ballarin *et al.* (28)
Ni–Al	Cl^-	Methanol-ethanol oxidation	1999	Ballarin *et al.* (29)
Mg–Al Zn-Cr	Quinone sulphonated, p-toluene, Cl^-	Ion accumulation, Retention capability	1998	Ballarin *et al.* (30)
Mg–Al	$[Fe(CN)_6]^{3-, 4-}$	A^{n-} adsorption, Mass transport	1998	Yao *et al.* (31)
Zn–Cr Zn–Al	$(FeC_{10}H_8S_2O_6^{2-})$, $(FeC_{10}H_9SO_3^-)$	Electrochemistry Reversibility	1998	Therias *et al.* (32)
Zn–Al Ni–Al Co–Al Mg–Al	$Cl—CO_3^{2-}$	Modified electrodes	1997	Qiu *et al.* (33)
Ni–Al Ni–Fe	$[Fe(CN)_6]^{4-}$ $[Mo(CN)_8]^{4-}$	Modified electrodes	1995	Qiu *et al.* (34)
Zn–Cr Zn–Al	Sulphonate	Modified electrodes	1995	Therias *et al.* (35)
Zn–Al	Metatungstate	Modified electrodes	1993/1991	Keita *et al.* (36, 37)

mortar in order to ensure a homogeneous distribution of the HTs. In all experiments, the paste was packed into a PVC tube with a geometric surface area of 0.031 m^2 and compacted using a piston. The electric connection was made through a copper wire. The electrodes were tested immediately after preparation, showing a reproducible electrochemical behavior. The reproducibility of the electrochemical response is due to both, the homogeneity of the paste and its stability throughout experimentation time. Indeed, renovation of the electrode surface after 8h of continuous use shows no changes in the electrode response.

2.3. Electrochemistry measurement and equipment

The electrochemical measurements were conducted in a three-electrode cell, using a 0.1M KOH (pH=12) solution prepared with deionized water as the support electrolyte. A graphite rod was used as the counter electrode (Alfa AESAR™; purity 99.9995 %), and the carbon paste electrode as the working electrode (preparation previously mentioned). A HgO/KOH electrode (0.926 vs SHE, filled with 0.1 M KOH) was used as reference. All the potentials are referred to the HgO/KOH scale. The potentials in the cell were imposed-controlled with a potentiostat PARC-283 coupled to a personal computer with the Corrware 2.2 software. The electrode surface was renewed after each sweep by removing approximately 3 mm of the paste out of the tube and polishing the new surface with a 600 mm Buhler paper. An average of three repetitions was done for each potential sweep rate to assess the reproducibility of the response. Cyclic voltammograms were started at the open circuit potential (OCP) of each HT modified electrode. Scans were recorded for both negative ($E_{-\lambda}$) and positive ($E_{+\lambda}$) inversion potentials. In this study, the Al^{3+} cations do not modify the reduction or oxidation process; therefore, we have only considered the influence of M^{2+} HT cations, Zn^{2+} and Mn^{2+}. Furthermore, the nitrate anions in the HTs promote a larger interlaminar distance than those obtained, for example, with CO_3^2 and, this facilitates a better diffusion of oxidative species with a higher sensitivity of conductivity measurements (38).

3. RESULTS AND DISCUSSION

3.1. Characterization of hydrotalcite materials

The XRD patterns of the HTs dried at 343 K, Figure 1, correspond to a hydrotalcite structure. The d_{003} distance is 8.8 Å, for the three samples; this distance is similar to the often reported value in nitrated HTs (16). However, some spinel phase is formed in the ternary (Zn-Mn)-Al HT, due to the oxidation of the reactants during preparation (17), probably induced by the microwave irradiation. The Mn samples, binary and ternary, show a characteristic brown color attributed to the oxidation process of Mn(II) to Mn(IV). Indeed, Mn(II) cations in an octahedral OH environment are slightly pink (as the hexa aqueous manganese (II) cations).

Lattice parameters *a* and *c* obtained from the hydrotalcite (110) and (003) reflections, respectively, are consistent with a hexagonal unit cell, Table 2. As Mn^{2+} ionic radius (0.80 Å) is larger than the Zn^{2+} ionic radius (0.74 Å) (4), cell parameter *a* is smaller in the Zn-Al HT (3.06 Å) than in the Mn-Al HT (3.15 Å). Indeed, Zn^{2+} and Mn^{2+} are inserted in the brucite layers of the corresponding samples. In the ternary sample, (Zn-Mn)-Al HT, the *a* parameter is also 3.15 Å with a molar nominal composition of Zn/Al = 0.2. However, Due to spinel presence, the HT composition is different

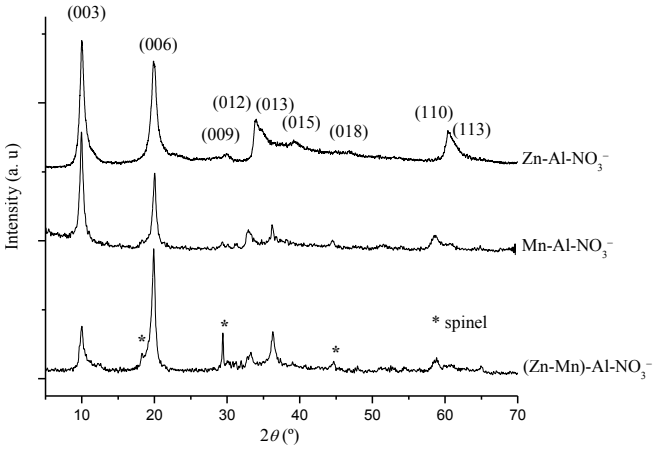

Figure 1. XRD patterns of nitrated HTs dried at 343 K.

as its nominal composition does not correspond to the formed compounds, as a high amount of Zn was incorporated into the spinel structure (12). For example, if the Végard law is used to determine the Zn/Mn ratio from the cell parameters, Table 2, the estimated hydrotalcite composition is $Zn_{0.06}Mn_{1.94}Al_{1.0}$, which corresponds to a Zn/Al value of 0.06.

As a conventional chemical analysis is bulk analysis, it does not separate the contribution of the HT and the spinel. Thus, the determination of the Zn/Al ratio in the HT through the Végard law will be used. Furthermore, (006) X-ray diffraction peak intensity is higher than the intensity of the (003) reflection in the (Zn-Mn)-Al-NO_3. To explain such difference, it has been proposed that a heavy metal (i.e. Zn) is located at the midpoint of the interlayer galleries (18-20).

If M^{2+}/Al bulk molar ratios determined by XRD (Végard Law) are compared to those obtained using EDX, Table 2, the ternary HT presents a molar ratio of Zn/Al = 0.57 (obtained by EDX) showing that the amount of Zn higher than the bulk one (XRD). Then, the homogeneity of this HT is not reached. The disagreement between these values can be understood, since microscopy is a local surface analysis, whereas X-ray diffraction corresponds to the bulk HT sample. The EDX analysis has to be strongly influenced by spinel particles. Therefore, the spinel composition can be estimated as follows $Zn_{1-x}Al_xMn_2O_4$, where $x \approx 0.57$ corresponding to the Al/Zn

Table 2. Cell parameters calculated according to the X-ray diffractograms of nitrated HTs and comparison of the Zn/Al and Mn/Al molar ratios obtained by XRD and EDX analysis.

M^{2+}–Al^{3+}	Cell parameters (by XRD)		Molar ratio comparison			
			Zn/Al		Mn/Al	
	a (Å, ±0.001)	*c* (Å, ±0.001)	XRD	EDX	XRD	EDX
Zn-Al	3.06	26.44	2.0	2.06	-	-
Mn-Al	3.15	26.64	-	-	2.0	1.94
(Zn-Mn)-Al	3.15	26.52	0.06	0.57	1.94	1.46

a and *c* parameters were obtained from $a = 2d_{110}$ and $c = 3d_{003}$. The XRD values correspond to HT whereas EDX values correspond to the sample surface analysis, no necessary HT.

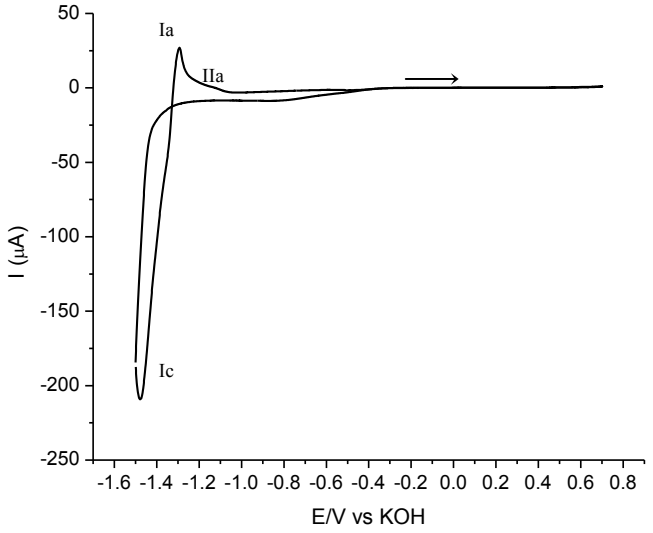

Figure 2. Cyclic voltammograms (v= 20 mVs^{-1}) of Zn-Al HT-CPE obtained in 0.1 M KOH. The scan was initiated from OCP (-0.1 V). Ia and IIa are the anodic peaks, Ic is the cathodic peaks.

spinel ratio (12) and it is covering part of the HT surface.

3.2. Cyclic Voltammetry characterization

A qualitative characterization of the Zn^{2+} and Mn^{2+} oxidation-states in the HTs was carried out for each sample using cyclic voltammetry (refer to the experimental section). Figure 2 shows a voltammogram obtained with the modified electrode Zn-Al HT in 0.1 M KOH solution. The scan was started from the OCP (-0.102 V) towards the anodic direction. As observed, no peaks are detected during the anodic process since Zn^{2+} cannot be longer oxidized. During the anodic scan, the charge transport is carried out by two mechanisms. The first one involves 'electron hopping' along the layers, while the second one is associated with the migration from the solution to the HT of the hydroxyl anions. Both mechanisms work to balance the polarization supplied to the CPE by the applied potential (35). On the other hand, when the scan is inverted to more negative potentials, a flux of cathodic current is verified on the electrode at negative potentials about -1.4 V, i.e. wave Ic.

Analysis of the supporting electrolyte (e.g. CPE without HT) confirms that this process can be related to the reduction of Zn^{2+} to Zn^0. The reaction occurring in this process could entail a partial dehydroxylation (OH_s^-) from the HT layers, arising in the formation of a mixed oxide (Al-O) containing Zn^0 as follows:

$$Al^{3+}-(OH^-)_2-Zn^{2+}+2e^- \leftrightarrow (Al^{3+}-O-Zn^0)+2OH_s^- \quad (1)$$

Note in Figure 2 that no peaks typically observed in voltammograms are recorded during the cathodic scan, even at more negative potentials (not shown). Not surprising, this is because Zn^{2+} reduction is not diffusive-controlled during the course of the experiment. Zinc ions are contained in the modified Zn-Al HT, thus, the rate controlling-step for the electronic transport is associated with the electron hopping mechanism along the HT layers. Other mechanisms such as dehydroxylation processes (OH_s^-) and the formation of zinc oxides (ZnO) due to the alkalinity of the supporting electrolyte could be also occurring. On the other hand, two peaks are detected in the anodic branch of the voltammogram. These processes have been assigned to the oxidation from Zn^0/Zn^{2+} (Ia) and Zn^0/ZnO (IIa). The ZnO formation is induced by changes in the interfacial pH between the modified HT electrode and the KOH solution.

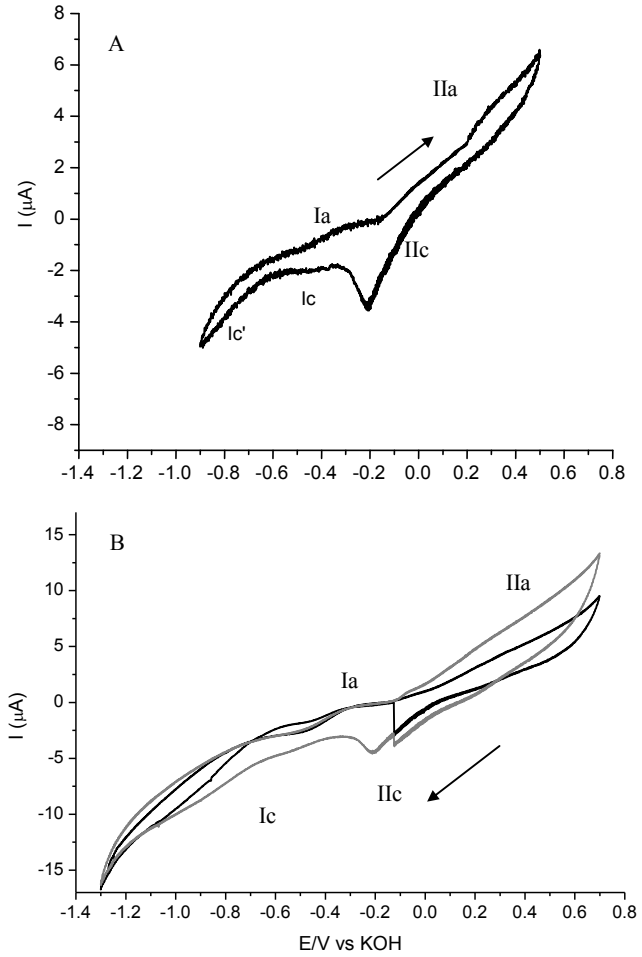

Figure 3. Cyclic voltammograms (v= 20 mVs^{-1}) of Mn-Al HT-CPE obtained in 0.1 M KOH. Scans were initiated from OCP (-0.12 V). A) In positive direction and B) in negative direction: first (black) and second (gray) cycles. Ia and IIa are the anodic peaks, Ic and IIc are the cathodic peaks.

Figure 3A shows a typical cyclic voltammogram started in the positive direction for the modified Mn-Al HT. As observed, the ionic current increases due to the following oxidation processes: Mn^{2+}/Mn^{3+} (Ia) and Mn^{3+}/Mn^{4+} (IIa). Roto *et al*. (7) have observed a similar Mn^{3+} oxidation phenomenon in a Mg-Mn carbonated HT electrode. Backward reactions are observed when the scan is switched to more negative potentials, e.g. peaks IIc, Ic. IIc would correspond to the Mn^{4+}/Mn^{3+} reduction, whereas the sluggish reduction Mn^{3+}/Mn^{2+} would be engaged in Ic. At potentials around -0.7 V, the reduction Mn^{2+}/Mn^0 occurs (Ic'). It is worth to mention

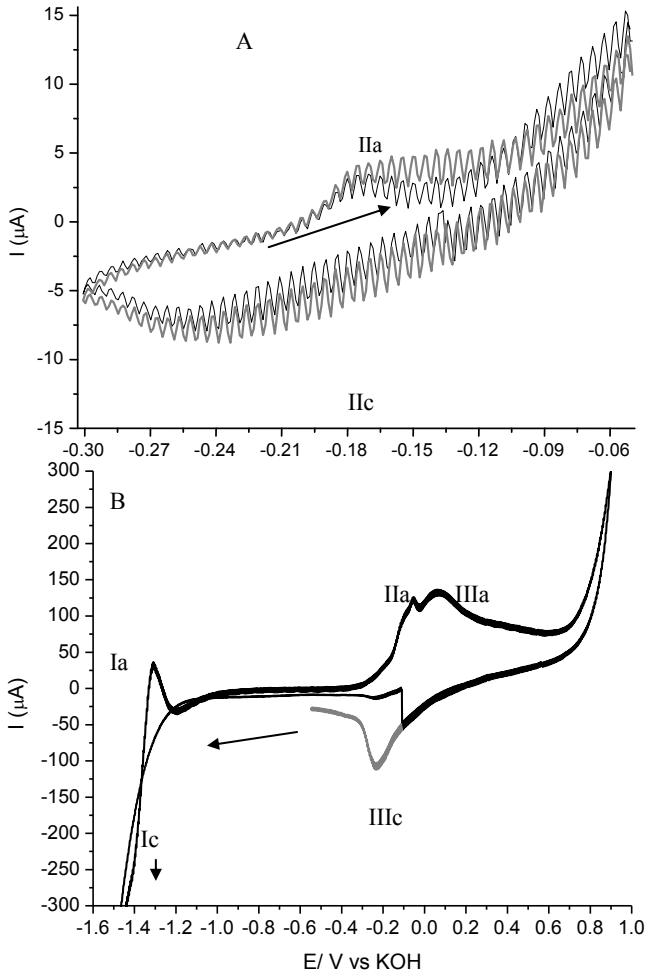

Figure 4. Cyclic voltammograms (v = 20 mVs^{-1}) of (Zn-Mn)-Al HT-CPE obtained in 0.1 M KOH. Scans were initiated from OCP in negative direction. A) $E_{-\lambda}$ = -0.3V and B) $E_{-\lambda}$= -2.1 V, first (black) and second (gray) cycles. Ia, IIa and IIIa are the anodic peaks, Ic, IIc and IIIc are the cathodic peaks.

that this reduction cannot be carried out when the scan is initiated in the positive direction. Presumably, intercalated Mn^{2+} in the HT layers is kinetically difficult to reduce, and therefore, it needs to be oxidized first. This finding is confirmed upon the formation of a peak in the cathodic branch of the voltammograms shown in Figure 3B, associated with the diffusive control of Mn^{4+} species. For this case, the formation of a mixed oxide probably occurs during the anodic scan as a result of the dehydroxylation process (OH_s^-):

$$Al^{3+} - (OH^-)_2 - Mn^{2+} + 2OH_s^- \leftrightarrow (Al^{3+} - O + Mn^{4+}) + 2H_2O + 2e^- \quad (2)$$

Although, the charge transport mechanism is similar to that one in the Zn-HT (electron hopping along the layers), the migration of anions is more accelerated due to the Mn^{4+}.

For the ternary system ((Zn-Mn)-Al HT), the oxidation-reduction mainly occurs on account of the Mn contained in the HT and the spinel structures. Figure 4A shows the reduction process Mn^{4+}/Mn^{3+} (peak IIc) for the first and second cycles. The process IIa describes the backward reaction. Note that this phenomenon was not observed in the modified Mn-Al HT. The Zn presents in the ternary sample leads to form the spinel $Zn_{0.43}Al_{0.57}Mn_2O_4$, previously identified by XRD (refer to section 3.1). Thus, the Mn^{4+} included in the spinel is reduced to Mn^{3+}, the total oxidation is guaranteed since the spinel shows a reversible process. If the potential becomes more positive, Figure 4B, the Zn oxidation process, peak Ia, is also observed and it is similar to that one observed in the modified Zn-Al HT (Figure 3). Likewise, two oxidation processes to form $Mn^{3+}$and Mn^{4+} are observed at more positive potentials, peaks IIa and IIIa respectively. They can be related to those observed in the Mn-Al sample (Figure 4). In fact, the corresponding cathodic peak, IIIc, can be attributed to the Mn^{4+} reduction.

Even though the open circuit voltage (OCV) for these HT samples was in the same order of magnitude, a variation was observed in their electrochemical behavior. For the binary samples, Zn-Al (Figure 2) and Mn-Al (Figure 3) HTs, the OCV values were -0.102 V and -0.143 V, respectively. The difference between these values has been attributed to the cation since the redox couple Zn^{2+}/Zn^0 presents a more negative potential in comparison with the redox couple for the Manganese species. On the other hand, the OCV for the ternary system was -0.014 V. Such difference can be related to the interactions arising between both cations present in the sample (e.g. Zn and Mn), which form a spinel phase. This remarkably modifies the electrochemical potential of the (Zn-Mn)-Al HT. Moreover, the different cations (M^{2+}) composition of the HTs can modify their electronic conductivity, as observed in Figures 3 and 4.

4. CONCLUSIONS

As shown by XRD and cyclic voltammetry performed under alkaline conditions (pH ≡12), the synthesized hydrotalcites differ in their stability, composition and structure. While the binary systems (Zn-Al and Mn-Al) present a typical hydrotalcite structure. The XRD pattern of the ternary system (Zn-Mn-Al) shows that one of the heavy metal atom (Zn) located at the midpoint of the HT galleries along with the formation of a spinel structure.

The hydrotalcites show different electrochemical stabilities in the cyclic voltammetry. The Zn-Al system turns out to be highly unstable; it decomposes irreversibly to the ZnO formation. On the contrary, the Mn-Al system shows a good electrochemical stability as the Mn ions oxidized and reduced reversibly. Lastly, the ternary system (Zn-Mn-Al) presents a different behavior in the sense that it cannot be understood as the addition of the two binary samples. These results could be explained in terms of a higher accessibility of manganese to the Redox processes, which is in agreement with the X-ray diffraction results, where the spinel structure containing Mn covers the HT. Hence, the main parameter is the Mn/Al ratio and not the crystalline structure. Still, the morphology due to hydrotalcite structure is lamellar and provides a regular distribution of manganese atoms interacting with zinc atoms through hydroxyl bridges. Cyclic voltammetry is a practical technique to qualitatively characterize the electrochemical behavior of the HTs and the different phenomena arising during their electron transfer. Likewise, it is useful to glimpse the kinetics of the exchange processes occurring during the dehydroxylation and oxidation processes inside the HTs

in order to evaluate the performance of these materials. More powerful techniques such as Electrochemical Impedance Spectroscopy will be the motivation of further studies to quantify the rate of these processes.

5. ACKNOWLEDGEMENTS

Authors thank to L. Baños and J. Guzmán for the XRD and EDX analysis. The financial support of CONACYT (project 79132) and PROMEP (project: 103.5/09/4194) are gratefully acknowledged.

REFERENCES

[1] Mousty Ch., Anal. Bioanal Chem., 396, 315 (2010).
[2] Walcarius A., Anal. Chim. Acta, 384, 1 (1999).
[3] Macha S.M., Fitch A., Microchim. Acta, 128, 1 (1998).
[4] Evans D.G., Slade R.C., T. Struct. Bond, 2006, 1.
[5] Cavani F., Trifiro F., Vaccari A., Catal. Today, 11, 173 (1991).
[6] Roto R., Villemure G., J. Electroanal. Chem., 527, 123 (2002).
[7] Roto R., Villemure G., Electrochem. Acta, 51, 2539 (2006).
[8] Roto R., Yu L., Villemure G., J. Electroanal. Chem., 587, 263 (2006).
[9] Grygar T., Marken F., Schröder U., Scholz F., Collect. Czech. Chem. Commun., 67, 163 (2002).
[10]Almeida C.M.V.B., Giannetti B.F., Electrochem. Comun., 4, 985 (2002).
[11]Olson C., Adams R.N., Anal. Chim. Acta, 22, 582 (1960).
[12]Sampieri A., Fetter G., Pfeiffer H., Bosch P., Solid State Sci., 9, 394 (2007).
[13]Radha A.V., Vishnu-Kamath P., Bull. Mater. Sci., 26, 661 (2003).
[14]Kühn T., Pöllman H., in 8th International Congress on Applied Mineralogy - ICAM 2004 [Eds.: M. Pecchio, F.R.D. d. Andrade], Aguas de Lindoia, Sao Paulo, Brasil, 2004, pp. 689.
[15]Rivera J.A., Fetter G., Bosch P., Mic. Mes. Mater., 89, 306 (2006).
[16]Miyata S., Clays Clay Miner., 31, 305 (1983).
[17]Aisawa S., Hirahara H., Uchiyama H., Takahashi S., Narita E., J. Solid State Chem., 167, 152 (2002).
[18]Beaudot P., DeRoy M.E., Besse J.P. Chem. Mater., 16, 935 (2004).
[19]del Arco M., Gutierrez S., Martin C., Rives V., Inorg. Chem., 42, 4232 (2003).
[20]Kooli F., Kosuge K., Tsunashima A., J. Solid State Chem., 118, 285 (1995).
[21]Scavetta E, Ballarin B., Berrettoni M., Carpani I., Giorgetti, M., Tonelli D., Electrochem. Acta, 51, 2129 (2006).
[22]Scavetta E., Berrettoni M., Nobili F., Tonelli D., Electroch. Acta, 51, 3305 (2005).
[23]Ballarin B., Berrettoni M., Carpani I., Scavetta E., Tonelli D., Anal. Chim. Acta, 538, 219 (2005).
[24]Carpani I., Berrettoni M., Ballarin B., Giorgetti M., Scavetta E., Tonelli D., Solid State Ionic, 168, 167 (2004).
[25]Shan D., Cosnier S., Mousty C. Biosensor Bioelec., 20, 390 (2004).
[26]Rojas Delgado R., Arandigoyen Vidaurre M., De Pauli C.P., Ulibarri M.A., Avena M.J., J. Colloid Interface Sci., 280, 431 (2004).
[27]Scavetta E., Berrettoni M., Seeber R., Tonelli D. Electroch. Acta, 46, 2681 (2001).
[28]Ballarin B., Morigi M., Scavetta E., Seeber R., Tonelli D., J. Electroanal. Chem., 492, 7 (2000).
[29]Ballarin B., Seeber R., Tonelli D., Vaccari A., J. Electroanal. Chem., 463, 123 (1999).
[30]Ballarin B., Gazzano M., Seeber R., Tonelli D., Vaccari A., J. Electroanal. Chem., 445, 27 (1998).
[31]Yao K., Taniguchi M., Nakata M., Shimazu K., Takahashi M., Yamagishi A., J. Electroanal. Chem., 457, 119 (1998).
[32]Therias S., Lacroix B., Schollhorn B., Mousty C., Palvadeau P., J. Electroanal. Chem., 454, 91 (1998).
[33]Qiu J., Villemure G., J. Electroanal. Chem., 428, 165 (1997).
[34]Qiu J., Villemure G., J. Electroanal. Chem., 395, 159 (1995).
[35]Therias S., Mousty C., Appl. Clay Sci., 10, 147 (1995).
[36]Keita B., Belhouari A., Nadjo L., J. Electroanal. Chem., 314, 345 (1991).
[37]Keita B., Belhouari A., Nadjo L., J. Electroanal. Chem., 355, 235 (1993).
[38]Scavetta E., Berrettoni M., Giorgetti M, Tonelli D., Electrochem. Acta, 47, 2451 (2002).